JOURNAL OF PROPULSION AND POWER
Vol. 10, No. 4, July–Aug. 1994

Hydrogen Recombination Kinetics and Nuclear Thermal Rocket Performance Prediction

Kyle K. Wetzel* and Wayne C. Solomon†
University of Illinois at Urbana-Champaign, Urbana, Illinois 61801

The rate constants for the hydrogen three-body collisional recombination reaction with atomic and molecular hydrogen acting as third bodies have been determined by numerous investigators during the past 30 yr, but these rates exhibit significant scatter. The discrepancies in the rate constants determined by different investigators are as great as two orders of magnitude in the temperature range of interest for nuclear thermal rocket (NTR) operation, namely, 2000–3300 K. The impact of this scatter on our ability to predict the specific impulse (I_{sp}) delivered by a 30-klbf NTR has been determined for chamber pressures and temperatures from, respectively, 20–1000 psia and 2700–3300 K. The variation in I_{sp} produced by using the different rate constants is as great as 10%, or 100 s. This variation also obscures the influence of chamber pressure on I_{sp}; using fast kinetics, low pressures yield significantly improved performance, while using slow or nominal kinetics, the pressure dependence of I_{sp} is negligible. Because the flow composition freezes at very small area ratios, optimization of the nozzle contour in the near-throat region maximizes recombination. Vibrational relaxation is found to produce negligible losses in I_{sp}.

Nomenclature

C_i	=	mass fraction of species i
C_p	=	specific heat at constant pressure
h, h_i	=	static enthalpy, global and species i
h_c	=	chamber enthalpy
I_{sp}	=	specific impulse
K_p	=	pressure-based equilibrium constant for dissociation of hydrogen = $\mathcal{R}Tk_d^M/k_r^M$
k_r^M, k_d^M	=	forward and reverse reaction rate constants for the three-body collisional recombination of hydrogen with species M acting as the third body
M	=	Mach number
$\mathcal{M}_i$	=	molecular weight of species i
p, p_c	=	static and chamber pressure
$\mathcal{R}$	=	universal molar gas constant
r^*	=	throat radius
T, T_c, T_w	=	static, chamber, and nozzle wall temperatures
v, v	=	velocity vector and magnitude of v
X_H	=	mole fraction of atomic hydrogen
ε_c, ε_e	=	nozzle contraction and expansion ratios
θ, θ_i	=	nozzle tangent angles downstream and upstream of the throat
θ_e	=	nozzle exit angle
κ_d, κ_u	=	nozzle radii of curvature downstream and upstream of the throat nondimensionalized with respect to r^*
ρ	=	flow density
$\dot{\rho}_i$	=	mass production rate of species i per unit volume

Introduction

DETERMINING the influence of hydrogen dissociation and recombination on the performance produced by nuclear thermal rockets (NTR) has been given high priority, but few studies of the importance of hydrogen recombination rates to NTR performance have been conducted.[1] The purpose of the current investigation is to isolate the importance of hydrogen recombination in predicting the performance of an NTR using hydrogen propellant.

Two teams of researchers have recently studied some aspects of hydrogen kinetics to NTR performance. Stubbs et al.[2] investigate adiabatic nozzle flows using Navier-Stokes solvers incorporating finite-rate chemical kinetics. Davidian and Kacynski[3] use a two-dimensional, nonequilibrium performance code incorporating the method of characteristics to study the effects of pressure, temperature, and thrust level on the specific impulse accounting for finite-rate kinetics. The latter researchers note that uncertainty exists in our current knowledge of the hydrogen recombination rates and report results for its influence on the specific impulse at one chamber temperature.

Hydrogen Chemistry

At NTR chamber temperatures (i.e., up to 3300 K), the only species present in significant concentrations in hydrogen propellant are neutral atoms and molecules of hydrogen, H and H_2, respectively. These species exist in equilibrium with each other through the following collisional reactions:

$$2H + H_2 \underset{k_d^{H_2}}{\overset{k_r^{H_2}}{\Leftrightarrow}} H_2 + H_2 \qquad \text{(Ia)}$$

$$2H + H \underset{k_d^{H}}{\overset{k_r^{H}}{\Leftrightarrow}} H_2 + H \qquad \text{(Ib)}$$

To determine values for $k_r^{H_2}$ and k_r^H, we consider the broad range of values presented in Refs. 4–31, including experimental and analytical investigations[9–12,14–20,22–31] and the recommendations of several reviewers,[4–8,13,21] most notably Baulch et al.[5] Warnatz,[7] and Cohen and Westberg.[8] These rates are presented graphically in Fig. 1. Since 1960, the only experiments which have been discarded are those which previous reviewers felt employed dubious experimental techniques or

Received April 29, 1993; presented as Paper 93-2499 at the AIAA 29th Joint Propulsion Conference and Exhibit, Monterey, CA, June 28–30, 1993; revision received July 29, 1993; accepted for publication Oct. 29, 1993.

*Graduate Student, Department of Aeronautical and Astronautical Engineering.

†Professor and Head of Department of Aeronautical and Astronautical Engineering, 306 Talbot Lab, MC-236, 104 S. Wright St.

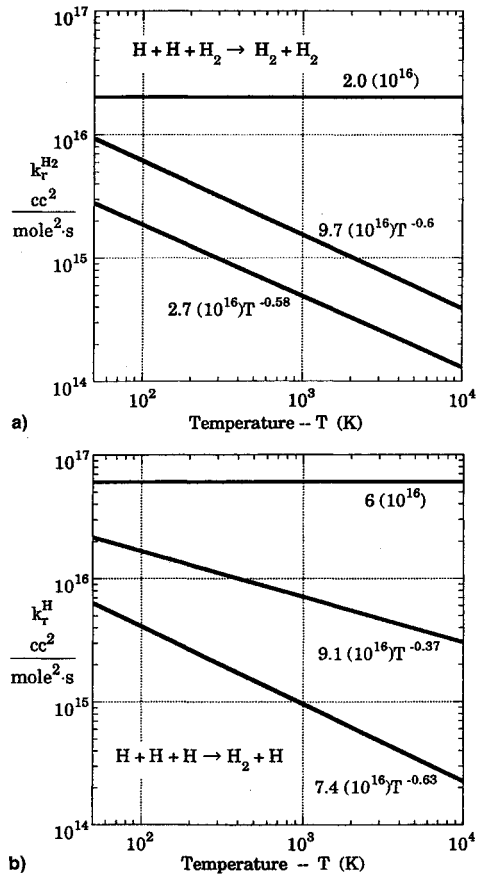

Fig. 1 Hydrogen recombination reaction rate constants: a) H_2 is the collision partner and b) H-atom is the collision partner.

procedures. We choose the following values for the "nominal" rates for Reaction (I):

$$k_r^{H_2} = 9.7 \times 10^{16} T^{-0.6} \frac{\text{cc}^2}{\text{mole}^2 \cdot \text{s}} \tag{1a}$$

$$k_r^{H} = 9.1 \times 10^{16} T^{-0.37} \frac{\text{cc}^2}{\text{mole}^2 \cdot \text{s}} \tag{1b}$$

The value for $k_r^{H_2}$ given by Eq. (1a) is recommended by several of the reviewers in the field.[5-8] Since no recent reviews recommend values for k_r^{H}, we propose the rate given by Eq. (1b) as the most reasonable fit to the data. The rates given by Eq. (1) are plotted as the heavy lines in Fig. 1.

It is apparent from Fig. 1 that significant scatter exists in the values determined for $k_r^{H_2}$ and k_r^{H}. This is greatest in the temperature range of interest for nuclear thermal rocket problems, namely, 2000–3300 K. Cohen and Westberg[8] and Baulch et al.,[5] claim that the uncertainty in their recommendations for log k_r^M are between ± 0.2 and ± 0.5 at all temperatures for M = Ar or H_2, meaning that the range of uncertainty in k_r is as great as an order of magnitude. Such statistical uncertainties are inappropriate for the purposes of our current investigation for several reasons:

1) Limited experimental data exists for H and H_2 as third bodies in the temperature range of most interest in this problem. In fact, fewer than 10 values exist for either rate constant between 1000–3000 K.

2) The reported uncertainty in $k_r^{H_2}$ of a factor of at most 10 excludes the values determined by several investigators, most notably Dixon-Lewis et al.,[16] Rosenfeld and Sugden,[23] Widawsky et al.,[25] Marshall,[29] and Wise and Ablow.[30] Although these investigations are among the older ones, none of the recent reviewers object to their procedures. Furthermore, it should be remembered that, although experimental determinations of k_r for inert third bodies such as argon have been conducted recently at high temperatures,[32] the last high-temperature investigation of $k_r^{H_2}$ or k_r^{H} was conducted by Hurle et al.[17] in 1969, and so all the data for the rates of interest are older. We give consideration to all the credible data in the temperature range of interest for NTRs, and this forces us to consider somewhat expanded bounds for this study.

3) The temperature dependence for k_r^{H} is not well known. The data for k_r^{H} appear to follow a very steep temperature dependence at high temperatures which when extrapolated to low temperatures does not match the reported low-temperature values. It should also be noted that none of the recent reviewers has recommended a value or uncertainty for k_r^{H}. Given this, we have determined the following upper and lower bounds on $k_r^{H_2}$ and k_r^{H}:

$$2.7 \times 10^{16} T^{-0.58} \leq k_r^{H_2} \leq 2 \times 10^{16} \frac{\text{cc}^2}{\text{mole}^2 \cdot \text{s}} \tag{2a}$$

$$7.4 \times 10^{16} T^{-0.63} \leq k_r^{H} \leq 6 \times 10^{16} \frac{\text{cc}^2}{\text{mole}^2 \cdot \text{s}} \tag{2b}$$

We recognize that our limits for $k_r^{H_2}$ are wider than those generally employed, but they represent our concerns about the scatter in the experimental data near 3000 K. They are also plotted as heavy lines in Fig. 1.

Performance Analysis and Nozzle Design

The following assumptions are made in the present analysis of reacting NTR nozzle flows:

1) The nozzle flow is steady and axisymmetric.

2) All component species of the gas obey perfect gas equations of state, although they are not necessarily calorically perfect (i.e., C_p is allowed to be temperature-dependent).

3) Diffusional processes are negligible.

4) The core flow outside a thin boundary layer is inviscid (i.e., potential).

5) Heat conduction is negligible in the core flow.

Given these assumptions, the governing equations for global continuity, conservation of momentum (the Navier-Stokes equations), and conservation of energy in the inviscid core are, respectively

$$\nabla \cdot (\rho v) = 0 \tag{3}$$

$$\rho (v \cdot \nabla) v = -\nabla p \tag{4}$$

$$h + (v^2/2) = h_c \tag{5}$$

where the enthalpy is

$$h = \sum_i C_i h_i \tag{6}$$

The continuity equation for species i is given by

$$\rho v \cdot \nabla C_i = \dot{\rho}_i \tag{7}$$

The species production rate $\dot{\rho}_i$ is dictated by the chemistry of the reacting propellant. Given reaction (I), it can be shown that the species production rate is[1]

$$\dot{\rho}_H = \dot{\rho}_{H_2} = \mathcal{M}_{H_2} \left(\frac{p}{\mathcal{R}T} \right)^3 [(1 - X_H) k_r^{H_2}(T) + X_H k_r^{H}(T)] \left[\frac{K_p(T)}{p} (1 - X_H) - X_H^2 \right] \tag{8}$$

Equations (3–8) can be reduced to a set of differential equations which are hyperbolic in the supersonic region of the nozzle. The method of characteristics is employed to solve the flowfield. The Two-Dimensional Kinetics (TDK) Nozzle Performance Computer Program,[33] which incorporates the method of characteristics, is widely used for analyzing nozzle flows.

The properties which strongly affect the performance of an NTR can be discerned from Eq. (8). The temperature, pressure, and rate constants appear explicitly. The rates of change in p and T are determined by the rate at which the flow expands, which is controlled by the geometry of the nozzle. Therefore, the factors which determine the rate of recombination are the chamber pressure and temperature, the nozzle geometry, and the magnitudes of the rate constants $k_r^{H_2}$ and k_r^H.

The key to maximizing the specific impulse delivered by an NTR is to maximize the dissociation of the H_2 in the chamber, thus maximizing the chamber enthalpy, which implies high temperatures and low pressures. It is also necessary to ensure recombination in the nozzle, which implies high pressures. Low pressures, however, restrict the thrust if reasonable engine size is to be maintained. Pressures on the order of one atmosphere produce no net system performance advantage, because the advantage gained in terms of specific impulse is negated by reducing the thrust-to-weight ratio significantly.[34] Given this, we consider chamber temperatures between 2700–3300 K, and chamber pressures between 20–1000 psia, to be feasible for NTRs which will likely be operating within the foreseeable future. These values are used in the current study.

The three nozzle contours selected in the present study are shown in Fig. 2, and the contour parameters are summarized in Table 1. All three have area ratios of 200:1; they differ in the radii of curvature upstream and downstream of the throat. The contours of the nozzles downstream of the throat are determined by choosing the parabolic contour option in TDK. The throat radii are shown in Table 2 for the chamber pressures investigated. For each p_c, the throat radius is selected so that nozzle 1 delivers a thrust of 30 klbf using nominal kinetics at 3100 K.

Viscosity and heat conduction through the nozzle wall will result in the formation of momentum and thermal boundary layers, thus reducing the delivered I_{sp}. A boundary-layer analysis module (BLM) can be coupled to TDK to determine the drag and heat losses.[33] It is necessary to determine the wall boundary conditions for input to BLM. Reference 34 presents a design for a 200:1 area ratio, radiation-cooled, carbon/carbon composite nozzle for use on an NTR with chamber conditions of 100 psia and 3300 K. A TDK analysis of this nozzle using an adiabatic wall produced an axial profile of the flow temperature, with which a heat transfer analysis of the nozzle was conducted, producing the axial wall temperature profile shown in Fig. 3.[34,35]

Using TDK and BLM, the nozzles shown in Fig. 2 are analyzed at the chamber pressures shown in Table 2, with T_c = 2700, 2900, 3100, and 3300 K, using the nozzle wall temperature profile shown in Fig. 3. The performance delivered by these nozzles is determined using fast, nominal, and slow kinetic rates as given by Eqs. (1) and (2). An equilibrium boundary-layer flow composition is used.

Table 1 Nozzle parameters

	Nozzle		
	1	2	3
ε_e	200	200	200
ε_c	16	16	16
κ_u	2	6	6
κ_d	1	10	40
θ_i	26 deg	40 deg	40 deg
θ	33 deg	25 deg	20 deg
θ_e	6.5 deg	6.5 deg	6.5 deg

Table 2 Throat radii

p_c, psia	r^*, in.
20	16.6
50	10.5
100	7.4
300	4.3
1000	2.3

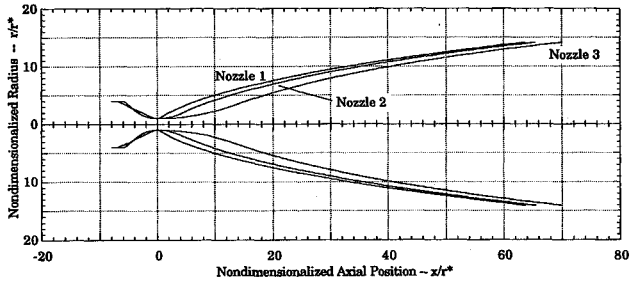

Fig. 2 Performance map for nozzle 3, accounting for kinetic, divergence, and boundary-layer losses, using nominal recombination rates.

Results

Stubbs et al.[2] investigate several nozzles using Navier-Stokes codes incorporating finite-rate kinetics. Their analyses use adiabatic nozzle walls. For comparison we determine the performance of the nozzle used by Stubbs et al. using TDK-BLM and an adiabatic wall at two chamber conditions which they studied. Table 3 summarizes the performance predicted by Stubbs and by the current study using the two different methods. The discrepancies of 3–5 s in I_{sp} as predicted by the two methods are fairly small.

Note that all further results presented in this article are for analyses using the cold wall temperature profile shown in Fig. 3. As is shown below, nozzle 3 yields superior performance to nozzle 2, which is superior to nozzle 1 at all operating conditions. Therefore, only results for nozzle 3 will be presented here, except for a comparison of the performance yielded by the three nozzles.

The specific impulse predicted for nozzle 3 as a function of the chamber conditions is shown in Fig. 4 using nominal hydrogen recombination kinetics. The specific impulse increases with chamber temperature as expected. At a midrange pres-

Table 3 Comparison of nozzle performance predicted using TDK-BLM and Navier-Stokes codes

Chamber pressure, atm	Area ratio	Thrust, klbf	I_{sp}, s: Present study	I_{sp}, s: Stubbs et al.[2]
6	240:1	5.4	1036	1041
10	100:1	98	1027	1024

T_c = 3200 K in all cases.

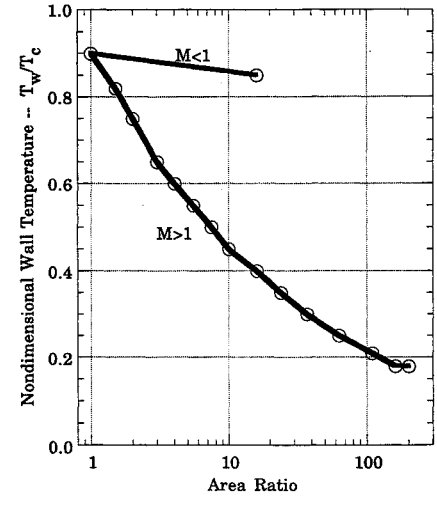

Fig. 3 Nozzle geometries analyzed.

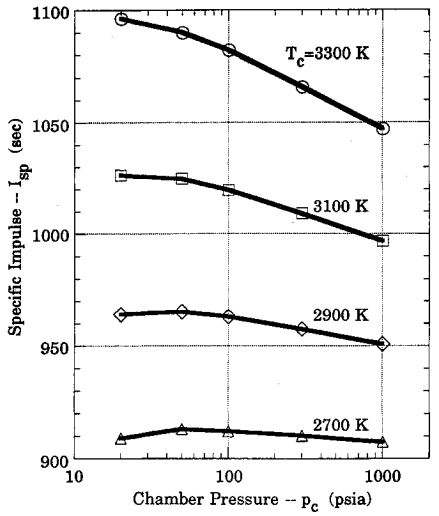

Fig. 4 Nozzle wall temperature profile.

sure of 100 psia, the temperature sensitivity of I_{sp} is about 0.25–0.3 s/K. Reference 34 concludes that a pressure of about 100 psia yields a nearly optimum combination of specific impulse and thrust-to-weight ratio. The NTR designed there uses a pebble bed reactor and nozzle 3 with chamber conditions of 100 psia and 3300 K to produce an I_{sp} of 1082 s, and a thrust-to-weight ratio of about 5. Table 4 summarizes the nozzle losses for this NTR. About one-third of the loss is attributable to each of the finite expansion, finite-rate kinetics, and boundary-layer losses. Only a negligible loss is attributed to divergence effects.

The pressure dependence of the specific impulse is slight at chamber temperatures of 2700–2900 K, varying no more than 15 s over the pressure range considered. At 3300 K, the I_{sp} rises about 50 s as the pressure is reduced from 1000 to 20 psia. The pressure of maximum performance increases as the temperature is reduced, lying at less than 20 psia for 3300 K and at 50–100 psia at 2700 K. The lack of significant pressure dependence in I_{sp} is a result of finite-rate kinetics and boundary-layer losses. Figure 5 illustrates these losses at T_c = 3300 K. As the pressure declines, the rates of recombination slow. Therefore, although the chamber enthalpy rises as the pressure drops, some of this advantage is negated by less recombination. Much of the energy that is put into dissociation at low pressures is lost. The boundary-layer losses also increase as the pressure declines and the temperature rises. This can be explained via the Reynolds numbers (Fig. 6). As the pressure drops and the temperature rises, the density of the propellant, and hence the Reynolds number declines, increasing the boundary-layer thickness and the I_{sp} losses.

Figure 5 also illustrates the differences in the kinetic and boundary-layer losses which result from using different values for the recombination rate constants. For example, at operating conditions of 100 psia and 3300 K, the losses relative to equilibrium performance due to finite-rate kinetics are only 15 s if one uses fast kinetic rates (see Fig. 5a). However, 60 s are lost if one uses the slow rates. The discrepancies are even greater at lower pressures, where the loss using slow kinetics approaches 170 s. Small differences in the boundary-layer losses also arise from using either the slow, nominal, or fast kinetics (see Fig. 5b), but these differences are less than 10 s.

The differences in the losses shown in Fig. 5 resulting from using different kinetic rates produce significant variations in the I_{sp} predicted for an NTP system. Figure 7 demonstrates the performance predicted for nozzle 3 accounting for finite-rate kinetics, divergence effects, and boundary-layer losses using not only the nominal recombination reaction rate but also the fast and slow rates at high temperatures. Using the nominal kinetics, a specific impulse of 1082 s is predicted for our NTR operating with a chamber pressure and temperature

Table 4 Nozzle loss summary

	I_{sp} loss, s	I_{sp}, s	Efficiency %
Ideal I_{sp}		1202	
Finite expansion loss	40	1162	96.7
Finite kinetics loss	41	1121	96.5
Divergence loss	3	1118	99.7
Boundary-layer loss	36	1082	96.8

T_c = 3000 K, p_c = 100 psia.

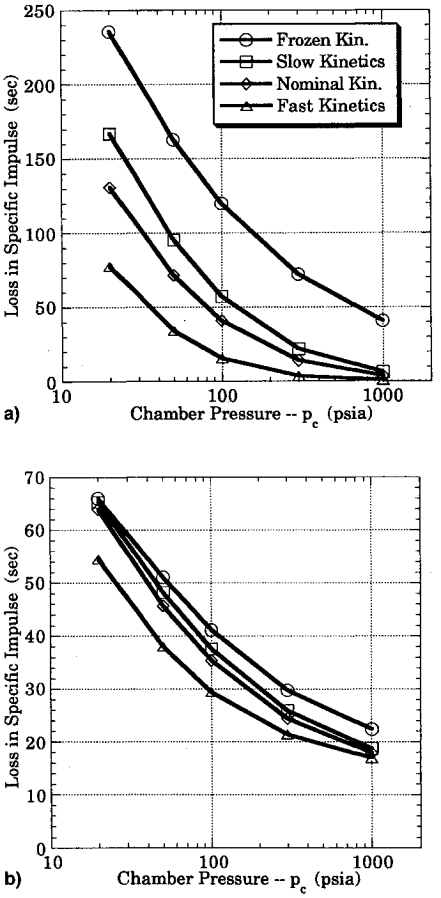

Fig. 5 Losses in the I_{sp} delivered by nozzle 3: a) kinetic losses in the potential flow and b) boundary-layer losses.

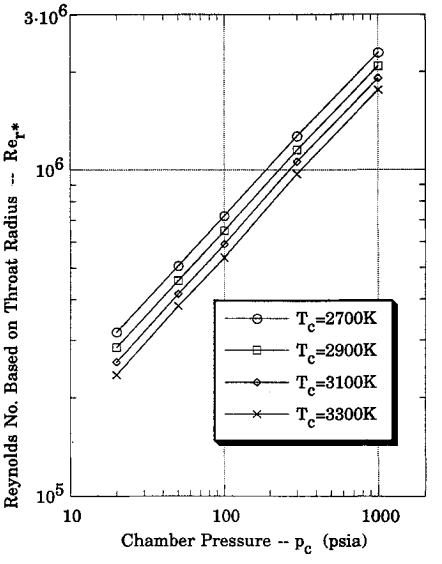

Fig. 6 Reynolds number based on the throat radius of nozzle 3.

of 100 psia and 3300 K. If the fast kinetics are used, then an I_{sp} of 1112 s is predicted, some 30 s better. On the other hand, using the slow kinetics reduces the delivered specific impulse to 1062 s, 20 s lower. Figure 8 summarizes the discrepancies in the specific impulse delivered by nozzle 3 over the entire range of chamber conditions produced by varying the kinetics used in performing the analysis. The discrepancies are significant at almost all chamber conditions, reaching a maximum of 100 s at p_c = 20 psia and T_c = 3300 K. At lower temperatures and high pressures, little dissociation exists, so the difference between equilibrium and frozen performance is not significant. For higher performance cases, as the temperature is raised and the pressure lowered, the dissociation increases and the kinetic effects become prominent.

The recombination kinetics can also obscure the influence of pressure on the specific impulse. If one uses slow recombination rates, lowering the pressure produces no benefits or even reduces the specific impulse. If nominal or fast kinetics are used, then lowering the pressure markedly improves the specific impulse. Without knowing the rates better, it is not possible to argue convincingly that either low- or high-pressure engines will deliver superior performance.

Figure 9 presents the difference in the specific impulse delivered by nozzles 1 and 3 using nominal kinetics at all chamber conditions analyzed. At 100 psia and 3300 K, the improvement is about 18 s. At lower pressures, as much as a 30 s improvement can be achieved. The only penalty to redesigning the nozzle is a slight increase in length, and therefore, weight. Reference 14 demonstrates that the weight penalty is far outweighed by the improvement in performance.

Figure 10 shows a direct comparison of the performances delivered by nozzles 1, 2, and 3, using both nominal (Fig. 10a) and fast kinetics (Fig. 10b). As noted above, if one uses nominal kinetics it appears that significant gains can be achieved

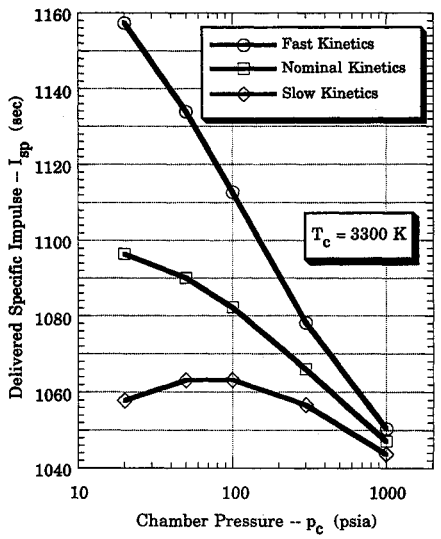

Fig. 7 Influence of recombination kinetics on the I_{sp}, accounting for divergence and boundary-layer losses.

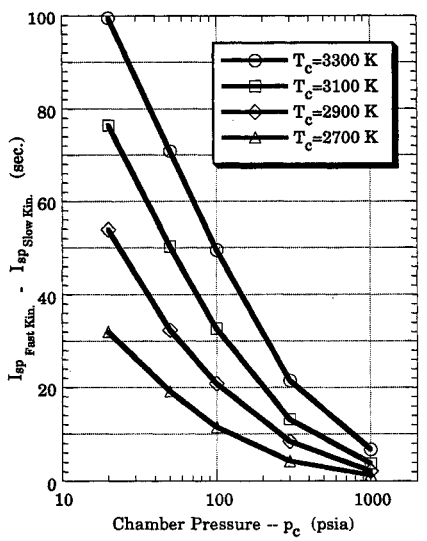

Fig. 8 Variation in I_{sp} of nozzle 3 due to recombination kinetics, accounting for divergence effects and boundary-layer losses.

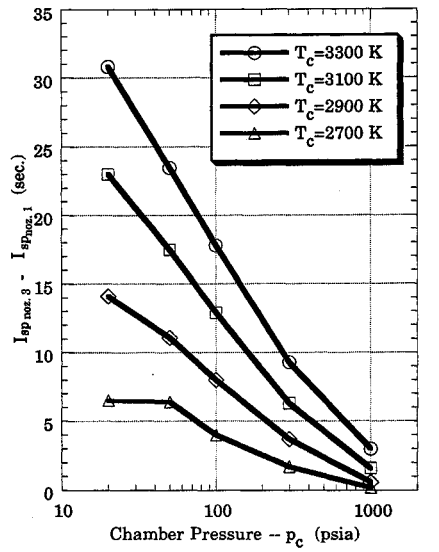

Fig. 9 Improvement in I_{sp} of nozzle 3 over nozzle 1, using nominal kinetics.

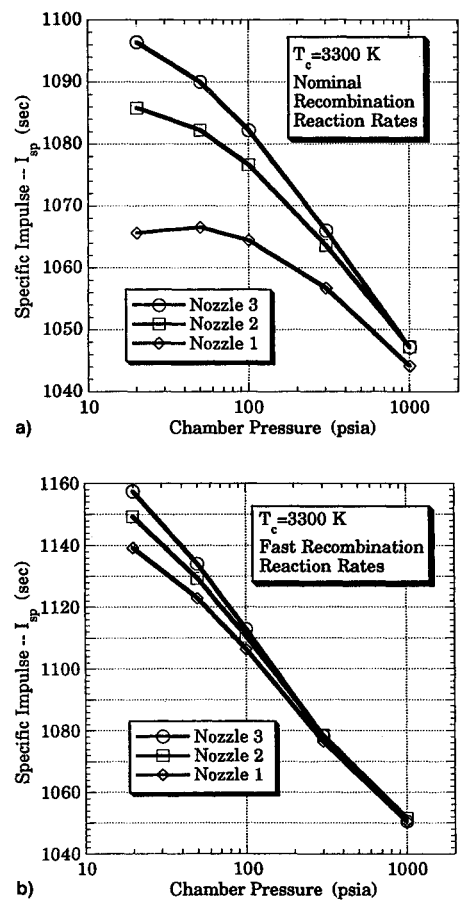

Fig. 10 Comparison of I_{sp} delivered by nozzles 1, 2, and 3, accounting for finite-rate kinetics, divergence effects, and boundary-layer formation: a) nominal recombination rates and b) fast recombination rates.

by redesigning the nozzle. However, if one uses fast kinetics, the gains appear to be negligible. Because the fast kinetics performance lies relatively near the equilibrium performance even in nozzle 1, there is little room for improvement, and little is achieved. The recombination kinetics can thus also obscure the nozzle designer's ability to optimize the contour. Without better knowledge of the kinetics, it is not possible to argue that redesigning the nozzle will definitely produce significant performance gains.

The influence of the kinetic rates on the recombination is alternatively presented in Figs. 11a and 11b. The former plots the atomic hydrogen mole fraction as a function of the local static temperature in the flow for the chamber conditions of 100 psia and 3300 K. In nozzle 1, using the slow kinetics, the flow composition freezes at about 9% mole fraction atomic hydrogen, whereas for the fast kinetics, it freezes at about 3.5%. For nozzle 3, the corresponding numbers are 7 and 2%. An approximate rule of thumb which evolves from the data is that each 1% mole fraction of atomic hydrogen which remains uncombined at the exit produces about 10 s of loss in specific impulse. The additional recombination in nozzle 3 releases energy which improves the I_{sp} by 15–25 s.

The area ratios at which the composition of the gas is freezing are barely past the circular arc contour downstream of the throat. For nozzle 1, the composition is frozen by area ratios of about 1.4:1, 1.8:1, and 3:1 downstream of the throat for, respectively, the slow, nominal, and fast kinetics. The corresponding area ratios for nozzle 3 are about 2:1, 2.5:1, and 3.5:1. The only way in which recombination can be significantly affected is to increase the radii of curvature of the contour upstream and downstream of the throat. Since the pressure drops as the area ratio increases, and since the drop in pressure eventually slows the recombination rate until the composition freezes, one can delay the freezing by slowing the rate of expansion near the nozzle throat. The atomic hydrogen continues to recombine at slightly larger area ratios in nozzle 3 than in nozzle 1 because the flow is expanding more slowly. Methods which attempt to optimize the nozzle contour downstream of the throat to enhance recombination are not useful, since the current results show that the composition is frozen in the downstream region.

Figure 12 plots the composition of the gas as a function of local static temperature in nozzle 3. The composition is essentially frozen at temperatures below 2000 K *regardless of the kinetics*. The flow composition freezes not because the temperature drops, but because the pressure drops. The two properties are related, however, and it simply turns out that in all cases the pressure falls low enough that the kinetics freeze at the point at which the temperature reaches about 2000 K. The significance of this is that the kinetic rates are only important at temperatures in this vicinity.

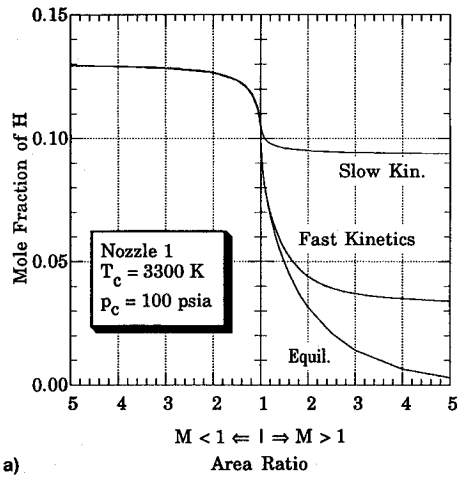

a)

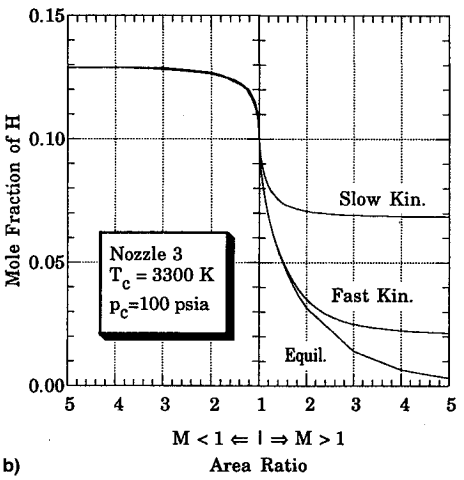

b)

Fig. 11 Axial profiles of atomic hydrogen mole fractions in the nozzle throat: a) nozzle contour 1 and b) nozzle contour 3.

Area Ratio Study

To study the influence of area ratio on nozzle performance, the area ratio of nozzle 1 is changed to 100, 150, 300, and 500, as shown in Ref. 35. The performance delivered by these nozzles with differing area ratios is again analyzed using the nominal kinetic rates. At 2700 K, the trends are as expected; the I_{sp} improves with increasing area ratio at all chamber conditions.[35] However, Fig. 13 shows that for a chamber temperature of 3300 K this is not true. At a chamber pressure of 1000 psia, the specific impulse is increased by 18 s by increasing the area ratio from 100 to 500. At 20 psia, the trend is reversed. The 100 and 150 area ratio nozzles deliver the best performance, followed by the 200, 300, and 500 area ratio nozzles in that order.

This enigmatic behavior is due to Reynolds effects, i.e., viscous losses. Most of the improvement in performance resulting from increased supersonic expansion is negated by growth in the boundary layer. The Reynolds number of the flow decreases as the chamber temperature increases and as the pressure declines, because in both cases the density of the flow is reduced (see Fig. 6). Therefore, as one increases the area ratio (and hence the nozzle diameter and length), the boundary-layer growth is more pronounced. The next generation of NTRs will have to produce an I_{sp} which can only be achieved with high temperatures and moderate pressures (e.g., 3300 K and 100 psia, respectively), where large area ratios do not produce significant improvements in I_{sp}.[35] This is why an area ratio of 200:1 is used in all the previous analysis.

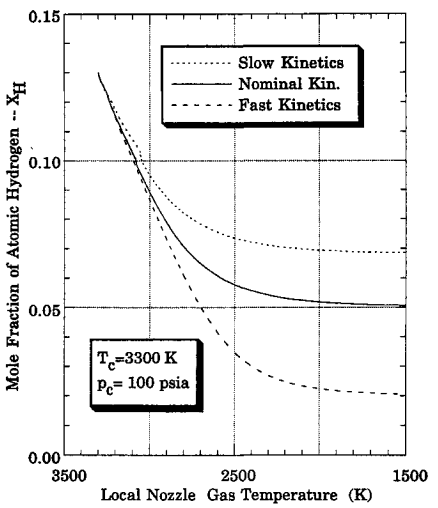

Fig. 12 Atomic hydrogen mole fraction as a function of the local static temperature in nozzle 3.

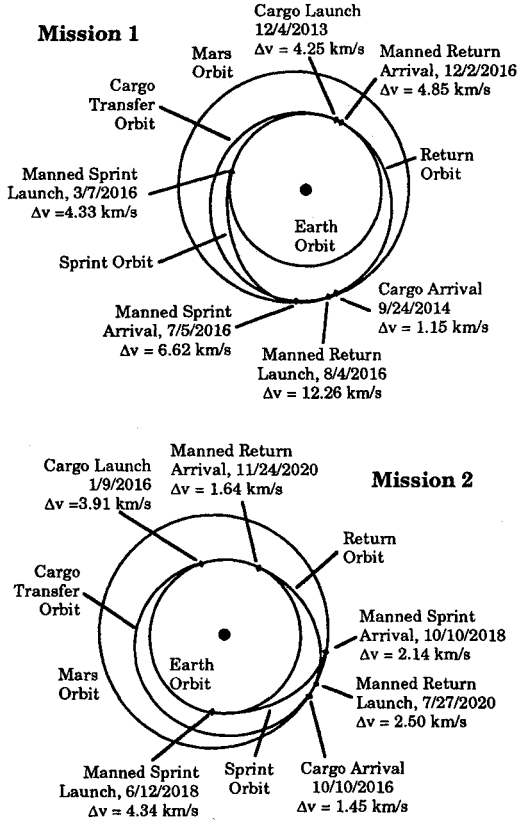

Fig. 13 Influence of the area ratio on the I_{sp} delivered by nozzle 1, accounting for finite-rate reaction kinetics, divergence effects, and boundary-layer losses.

Vibrational Relaxation Analysis

Nonequilibrium vibrational relaxation of molecular hydrogen could feasibly reduce the specific impulse of a nuclear thermal rocket by locking up energy in higher vibrational states. To investigate this, we perform a one-dimensional, finite-rate kinetic analysis, treating molecular hydrogen in each vibrational state v as a separate species, namely $H_2(v)$, where $H_2(0)$ is the ground vibrational state. It can be shown that it is necessary to track at least four excited vibrational states of molecular hydrogen (i.e., $v = 0$–4).[1] Reaction (I) becomes

$$2H + M \underset{{}^{v}k_d^M}{\overset{{}^{v}k_r^M}{\Longleftrightarrow}} H_2(v) + M \qquad \text{(II)}$$

where M can be H or $H_2(v)$. The values of ${}^{v}k_r^M$ for $v = 0$–4 for reaction (II) are selected to maintain the global recombination rate the same as in the previous analyses where individual v states are not tracked. That is, the net recombination produced by reactions (II) for all v states is the same as that produced by reaction (I).

In addition, however, one must follow the V-T and exchange reactions among the vibrationally excited states, listed below in that order:

$$H_2(v) + M \underset{}{\overset{k_{3,v}^M}{\Longleftrightarrow}} H_2(v-1) + M \qquad \text{(III)}$$

$$H + H_2(v) \underset{}{\overset{k_{4,v}^{v'}}{\Longleftrightarrow}} H_2(v') + H(v' > v) \qquad \text{(IV)}$$

where the rates for reactions (III) and (IV) are[1,36]

$$k_{3,v}^{H} = 2 \times 10^{13} e^{-2720/RT} \frac{cc}{mole \cdot s} \qquad (9)$$

Table 5 Hydrogen exchange reaction activation energies

v	v'	$E_a^{v,v'}$ kcal/mole
0	0	9.9
0	1	21.8
0	2	33.0
1	1	9.9
1	2	21.1
1	3	31.7
2	2	9.9
2	3	20.5
2	4	30.4
3	3	9.9
3	4	10.8

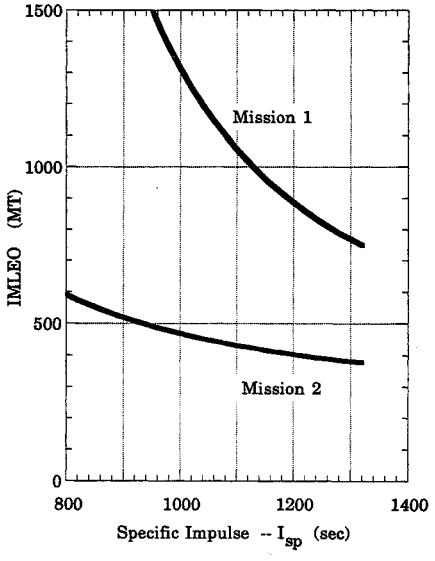

Fig. 14 Loss in the I_{sp} of nozzle 1 due to vibrational relaxation.

$$k_{3,v}^{H_2} = v \cdot 10^{-3} T^{4.3} \frac{cc}{mole \cdot s} \qquad (10)$$

$$k_{4,v}^{v'} = 2.26 \times 10^{14} \exp(-E_a^{v,v'}/RT) \frac{cc}{mole \cdot s} \qquad (11)$$

Values for $E_a^{v,v'}$ are shown in Table 5.

Figure 14 indicates that vibrational relaxation does not cause significant loss in performance. All the points in this graph represent less than 1 s loss in I_{sp}. It is, therefore, arguable that such losses are negligible next to the other uncertainties in the calculation. The losses tend to peak at intermediate temperatures. The reason for this is that as the temperature is increased from 2700 to 3100 K, the higher vibrational states of the molecular hydrogen first become excited. As the temperature is increased further, however, dissociation of the molecular hydrogen actually reduces the mole fractions of vibrationally excited hydrogen, so the associated losses also decline. The losses increase as the pressure declines, because the relaxation rates slow. At high temperatures, as the pressure drops the dissociation becomes so significant that relatively little of the hydrogen is in the vibrationally excited molecular state, so the losses experienced at moderate pressures are actually greater than those experienced at lower pressures.

Conclusions and Recommendations

Based on this investigation, the following conclusions can be drawn:

1) The I_{sp} predicted for NTRs varies as much as 10%, or 100 s, depending upon whether one uses recombination kinetics at the upper or lower bounds.

2) The recombination kinetics obscures the influence of chamber pressure on the I_{sp} of NTRs. (Using fast kinetics, low pressures yield dramatically improved performance, or using slow kinetics, the pressure dependence of I_{sp} is negligible.) Without better knowledge of the reaction rates, it is not possible to definitively establish that high- or low-pressure systems are preferable.

3) Optimization of a nozzle contour to ensure recombination must occur in the throat region, because the flow composition freezes at area ratios of between 3.5:1–1.5:1.

4) The recombination kinetics hampers the nozzle designer's ability to optimize the nozzle geometry. Using nominal rates, significant advantages accrue from lengthening the throat region. Using fast rates, the gains achieved by such a redesign are negligible.

5) The flow composition is essentially frozen at local static temperatures below 2000 K, so the kinetics at these temperatures are not as important.

6) The specific impulse delivered by a nozzle decreases with increasing area ratio when operating at high chamber temperatures and low pressures because of boundary-layer growth.

7) Including the kinetics for vibrational relaxation produces only small losses in I_{sp}.

The recombination reaction rate constants for hydrogen should be more accurately determined experimentally in the temperature range 2000–3500 K. Particular importance is placed on the lower end of this range, given the paucity of data there, and on determining the reaction rate for atomic hydrogen as the third body.

References

[1]Wetzel, K. K., "An Investigation of the Influence of Hydrogen Recombination Kinetics on the Performance of Nuclear Thermal Rocket Nozzles," M.S. Thesis, Univ. of Illinois at Urbana-Champaign, Urbana, IL, 1993.

[2]Stubbs, R. M., Kim, S. C., and Papp, J. L., "Analysis of Nuclear Thermal Propulsion Systems Using Computational Fluid Dynamics," 10th Symposium on Space Nuclear Power and Propulsion, Jan. 1993; also Kim, S., and Stubbs, R., "Numerical Study of Low Pressure Nuclear Thermal Rockets," AIAA Paper 92-3815, July 1992; and also Stubbs, R. M., Kim, S. C., and Benson, T. J., "Computational Fluid Dynamics Studies of Nuclear Rocket Performance," AIAA Paper 91-3577, Sept. 1991.

[3]Davidian, K. O., and Kacynski, K. J., "Analytical Study of Nozzle Performance for Nuclear Thermal Rockets," AIAA Paper 91-3578, Sept. 1991.

[4]Oldenborg, R., personal communication, Los Alamos National Lab., Los Alamos, NM, 1992.

[5]Baulch, D. L., et al., "Evaluated Kinetic Data for Combustion Modelling," *Journal of Physical and Chemical Reference Data*, Vol. 21, No. 3, 1992, pp. 411–735.

[6]Harradine, D. M., Lyman, J. L., Oldenborg, R. C., Schott, G. L., and Watanabe, H. H., "Hydrogen/Air Combustion Calculations: The Chemical Basis of Efficiency in Hypersonic Flows," *AIAA Journal*, Vol. 28, No. 10, 1990, pp. 1740–1744.

[7]Warnatz, J., "Rate Coefficients in the C/H/O System," *Combustion Chemistry*, Springer-Verlag, New York, 1984, pp. 197–360.

[8]Cohen, N., and Westberg, K. R., "Chemical Kinetic Data Sheets for High-Temperature Chemical Reactions," *Journal of Physical and Chemical Reference Data*, Vol. 12, No. 3, 1983, pp. 531–590.

[9]Levitskii, A. A., and Polak, L. S., "Study of the Recombination Reaction H + H + H'H_2 + H by the Classical Trajectories Method," *High Energy Chemistry*, Vol. 12, No. 4, 1978, pp. 245–248.

[10]Lynch, K. P., Schwab, T. C., and Michael, J. V., "Lyman-α Absorption Photometry at High Pressure and Atom Density Kinetic Results for H Recombination," *International Journal of Chemical Kinetics*, Vol. 8, 1976, pp. 651–671.

[11]Walkauskas, L. P., and Kaufman, F., "Gas Phase Hydrogen Atom Recombination," 15th Symposium (International) on Combustion, Tokyo, Aug. 1974; also Trainor, D. W., Ham, D. O., and Kaufman, F., "Gas Phase Recombination of Hydrogen and Deuterium Atoms," *Journal of Chemical Physics*, Vol. 58, No. 10, 1973, pp. 4599–4609; and also Ham, D. O., Trainor, D. W., and Kaufman, F., "Gas Phase Kinetics of H + H + H_2'$2H_2$," *Journal of Chemical Physics*, Vol. 53, No. 10, 1970, pp. 4395, 4396.

[12]Shui, V. H., "Thermal Dissociation and Recombination of Hydrogen According to the Reactions H_2 + H'H + H + H," *Journal of Chemical Physics*, Vol. 58, No. 11, 1973, pp. 4868–4879.

[13]Baulch, D. L., Drysdale, D. D., Horne, D. G., and Lloyd, A. C., *Evaluated Kinetic Data for High Temperature Reactions, Vol. 1. Homogeneous Gas Phase Reactions of the H_2-O_2 System*, Butterworths, London, 1972.

[14]Bennett, J. E., and Blackmore, D. R., "Rates of Gas-Phase Hydrogen-Atom Recombination at Room Temperature in the Presence of Added Gases," 13th Symposium (International) on Combustion, Salt Lake City, UT, Aug. 1971; also Bennett, J. E., and Blackmore, D. R., "Gas-Phase Recombination Rates of Hydrogen and Deuterium Atoms," *Journal of Chemical Physics*, Vol. 53, No. 10, 1970, pp. 4400, 4401; and also Bennett, J. E., and Blackmore, D. R., "The Measurement of the Rate of Recombination of Hydrogen Atoms at Room Temperature by Means of E.S.R. Spectroscopy," *Proceedings of the Royal Society of London, Series A*, Vol. 305, 1968, pp. 553–574.

[15]Roberts, R. E., and Bernstein, R. B., "Rate Constant for Deuterium Atom Recombination Calculated by the Orbiting Resonance Theory," *Chemical Physics Letters*, Vol. 6, No. 4, 1970, pp. 282–284; also Roberts, R. E., Bernstein, R. B., and Curtiss, C. F., "Resonance Theory of Termolecular Recombination Kinetics: H + H + M'H_2 + M," *Journal of Chemical Physics*, Vol. 50, No. 12, 1969, pp. 5163–5176.

[16]Dixon-Lewis, G., "Flame Structure and Flame Reaction Kinetics V. Investigation of Reaction Mechanism in a Rich Hydrogen + Nitrogen + Oxygen Flame by Solution of Conservation Equations," *Proceedings of the Royal Society of London, Series A*, Vol. 317, 1970, pp. 235–263; also Dixon-Lewis, G., Sutton, M. M., and Williams, A., "Some Reactions of Hydrogen Atoms and Simple Radicals at High Temperatures," 10th Symposium (International) on Combustion, Cambridge, England, UK, 1965; and also Dixon-Lewis, G., Sutton, M. M., and Williams, A., "The Kinetics of Hydrogen Atom Recombination," *Discussions of the Faraday Society*, No. 33, 1962, pp. 205–212.

[17]Hurle, I. R., Jones, A., and Rosenfeld, J. L. J., "Shock-Wave Observations of Rate Constants for Atomic Hydrogen Recombination from 2500 to 7000°K: Collisional Stabilization by Exchange of Hydrogen Atoms," *Proceedings of the Royal Society of London, Series A*, Vol. 310, 1969, pp. 253–276.

[18]Larkin, F. S., "Homogeneous Rate of Recombination of Hydrogen Atoms," *Canadian Journal of Chemistry*, Vol. 46, 1968, pp. 1005–1015; also Larkin, F. S., and Thrush, B. A., "The Kinetics of Hydrogen-Atom Recombination," 10th Symposium (International) on Combustion, Cambridge, England, UK, 1965; and also Larkin, F. S., and Thrush, B. A., "Recombination of Hydrogen Atoms in the Presence of Atmospheric Gases," *Discussions of the Faraday Society*, No. 34, 1964, pp. 112–117.

[19]Jacobs, T. A., Giedt, R. R., and Cohen, N., "Kinetics of Hydrogen Halides in Shock Waves. II. A New Measurement of the Hydrogen Dissociation Rate," *Journal of Chemical Physics*, Vol. 47, No. 1, 1967, pp. 54–57.

[20]Hurle, I. R., "Measurements of Hydrogen-Atom Recombination Rates Behind Shock Waves," 11th Symposium (International) on Combustion, Berkeley, CA, 1967.

[21]Heicklen, J., "Gas-Phase Chemistry of Re-Entry," *AIAA Journal*, Vol. 5, No. 1, 1967, pp. 4–15.

[22]Russo, A. L., Hall, J. G., and Lordi, J. A., Cornell Univ., Rept. AD-1689-A-4, Ithaca, NY, 1964.

[23]Rosenfeld, J. L. J., and Sugden, T. M., "Burning Velocity and Free Radical Recombination Rates in Low Temperature Hydrogen Flames. II—Rate Constants for Recombination Reactions," *Combustion and Flame*, Vol. 8, March 1964, pp. 44–50.

[24]Kretschmer, C. B., and Petersen, H. L., "Kinetics of Three-Body Atom Recombination," *Journal of Chemical Physics*, Vol. 39, No. 7, 1963, pp. 1722–1778.

[25]Widawsky, A., Oswalt, L. R., and Harp, J. L., "Experimental Determination of the Hydrogen Recombination Constant," *ARS Journal*, Vol. 32, No. 12, 1962, pp. 1927–1929.

[26]Sutton, E. A., "Measurement of the Dissociation Rates of Hydrogen and Deuterium," *Journal of Chemical Physics*, Vol. 36, No. 11, 1962, pp. 2923–2931.

[27]Rink, J. P., "Shock Tube Determination of Dissociation Rates of Hydrogen," *Journal of Chemical Physics*, Vol. 36, No. 1, 1962, pp. 262–265.

[28]Patch, R. W., "Shock-Tube Measurement of Dissociation Rates of Hydrogen," *Journal of Chemical Physics*, Vol. 6, No. 7, 1962, pp. 1919–1924.

[29]Marshall, T. C., "Studies of Atomic Recombination of Nitrogen,

Hydrogen, and Oxygen by Paramagnetic Resonance," *Physics of Fluids*, Vol. 5, No. 7, 1962, pp. 743–753.

[30]Wise, H., and Ablow, C. M., "Diffusion and Heterogeneous Reaction. IV. Effects of Gas-Phase Reaction and Convective Flow," *Journal of Chemical Physics*, Vol. 35, No. 1, 1961, pp. 10–18.

[31]Avramenko, L. I., and Kolesnikova, R. V., "The Determination of the Rate Constants of the Simple Reactions of Hydrogen Atoms," *Bulletin of the Academy of Sciences of the USSR*, No. 11, 1961, pp. 1839–1843.

[32]Du, H., and Hessler, J. P., "Rate Coefficient for the Reaction H + O_2 OH + O: Results at High Temperatures, 2000 to 5300 K," *Journal of Chemical Physics*, Vol. 96, No. 2, 1992, pp. 1077–1092.

[33]Nickerson, G. R., and Coats, D., "Two-Dimensional Kinetics (TDK) Nozzle Performance Computer Program," Software and Engineering Associates, NASA Contract NAS8-36863, Carson City, NV, 1988.

[34]Willmes, G., et al., "A High- I_{sp} Nuclear Thermal Rocket for Space Exploration," Univ. of Illinois at Urbana-Champaign, Repts. UILU 93-0505 and AAE 93-05, Urbana, IL, Dec. 1992.

[35]Wetzel, K. K., and Solomon, W. C., "Effect of the Uncertainty in Hydrogen Recombination Kinetics on NTR Performance Prediction," AIAA Paper 93-2499, June 1993.

[36]Cohen, N., and Bott, J. F., "Review of Rate Data for Reactions of Interest in HF and DF Lasers," Air Force Weapons Lab., Air Force Systems Command, Rept. SD-TR-82-86, Albuquerque, NM, 1982.